
*Research article***A noise-tolerant zeroing neural network with fixed-time convergence for solving multi-linear systems with nonsingular \mathcal{M} -tensors****Ruijuan Zhao^{1,*}, Mengyao Li¹, Tingjia Liu² and Shu-Xin Miao²**¹ School of Information Engineering and Artificial Intelligence, Lanzhou University of Finance and Economics, Lanzhou 730101, China² School of Mathematics and Statistics, Northwest Normal University, Lanzhou 730070, China*** Correspondence:** Email: zhaobin7755382@163.com.

Abstract: Multi-linear systems play a crucial role in various practical applications such as high-dimensional partial differential equations (PDEs), signal processing, and high-order statistics. In this paper, we propose a noise-tolerant zeroing neural network (NTZNN) model with fixed-time convergence activated by a new nonlinear activation function for solving multi-linear systems with nonsingular \mathcal{M} -tensors. The detailed theoretical analysis demonstrates that the NTZNN model is stable in the sense of Lyapunov stability theory and achieves fixed-time convergence with or without the presence of noises. Furthermore, compared with existing neural network models, the proposed NTZNN model significantly improves the convergence rate while maintaining noise tolerance. Numerical experiments further show the effectiveness and superiority of the proposed NTZNN model.

Keywords: zeroing neural network; multi-linear systems; fixed-time convergence; noise-tolerant; nonsingular \mathcal{M} -tensors

AMS subject classifications: 15A69, 65F15, 68W25

1. Introduction

Multi-linear systems, as a special type of tensor equation, have many applications in various fields of engineering and scientific computing, such as evolutionary game dynamics, data mining, numerical partial differential equations, and tensor complementarity problems [1–4], and therefore have gained significant attention in recent years. A multi-linear system can be expressed as

$$\mathcal{A}x^{m-1} = b, \quad (1.1)$$

where $\mathcal{A} = (a_{i_1 i_2 \dots i_m})$ is an m th-order n -dimensional tensor, $x = (x_1, x_2, \dots, x_n)^T$ is an unknown vector, b is an n -dimensional vector, and $\mathcal{A}x^{m-1}$ is an n -dimensional vector with its i th element defined by

$$(\mathcal{A}x^{m-1})_i = \sum_{i_2, \dots, i_m=1}^n a_{i i_2 \dots i_m} x_{i_2} \cdots x_{i_m}, \quad i = 1, 2, \dots, n.$$

Ding and Wei [1] pointed out that the multi-linear system (1.1) has a unique positive solution when the coefficient tensor \mathcal{A} is a nonsingular \mathcal{M} -tensor and the right-hand side b is a positive vector. Meanwhile, they extended several classical iterative methods, including the Jacobi method, the Gauss–Seidel method, and the Newton method, to solve such multi-linear system. After that, many efficient iterative algorithms have been developed to solve the multi-linear system (1.1) with the coefficient tensor \mathcal{A} being nonsingular (symmetric or semi-symmetric) \mathcal{M} -tensor, such as Newton-type methods [5,6], the homotopy method [7], splitting iterative methods [8–10], preconditioned splitting iterative methods [11,12], Levenberg–Marquardt (LM) method [13]. Additionally, Liang et al. presented a two-step accelerated LM method [14] and an ADMM-type method [15] to solve the multi-linear system (1.1) with nonsingular tensors. However, these numerical methods often entail high computational costs and pose challenges in meeting the real-time requirements of practical applications.

Neural network approaches [16], as a parallel optimization approach, have significant advantages in distributed storage, hardware implementation, and high-speed parallel processing. They have been successfully applied in solving nonlinear optimization problems [17–20], constrained quadratic minimax optimization problems [21], linear equations [22–24], and non-linear equations [25–27], Drazin inverse [28,29], generalized inversion [30,31], matrix inversion [32,33], Sylvester equations [34–36], sparse signal reconstruction [37,38], and so on. Inspired by the zeroing neural network (ZNN) approaches [39], Wang et al. [40] designed a continuous time neural network (CTNN) model to solve the multi-linear system (1.1) with \mathcal{A} being an \mathcal{M} -tensor, which is obtained by utilizing the error monitoring functions $\varepsilon(t) = \mathcal{A}x(t)^{m-1} - b$ and a linear activation function. They indicated that compared with the Newton method [1], the CTNN method can effectively improve the computational efficiency. However, CTNN has the imperfection of infinite-time convergence and low convergence rate due to its linear activation function. For this reason, based on the ZNN model, Wang et al. [41] proposed three ZNN models by using three types of nonlinear activation functions named simplified, extended, and piecewise activation functions, respectively. Compared with the CTNN model, these models achieve finite-time convergence and are more effective in solving the multi-linear system (1.1) with \mathcal{M} -tensors. Different from the above-mentioned CTNN and ZNN models, Liu et al. [42] proposed a noise-suppressing discrete-time neural dynamics (NSDTND) model for solving time-dependent multi-linear \mathcal{M} -tensor equations, which are robust against noise. However, the NSDTND model is only effective when the order and dimension of the coefficient tensor of (1.1) are very small. Besides, Wang et al. utilized norm-based error monitoring functions $\frac{1}{2}\|\varepsilon(t)\|_2^2$ and different types of activation functions to establish the gradient neural network (GNN) approach for solving the multi-linear system (1.1) with non-singular tensors and \mathcal{KS} tensors in [43,44], respectively. Compared with the GNN model, the ZNN model has significant advantages in terms of global and exponential convergence properties [45]. Therefore, this paper is mainly concerned with neural network approaches based on the ZNN model. Additionally, noise disturbances are inevitable and ubiquitous in practical life, including external disturbance, model uncertainty, or computational error. However, the above-

mentioned CTNN [40] and ZNN models [41] do not take into account the impact of noise disturbances, and so the convergence of these models cannot be guaranteed in the presence of noise disturbances. Furthermore, these models have infinite-time/finite-time convergence, resulting in excessively long convergence times if the initial state value is not well chosen.

To address the aforementioned limitations, this paper proposes a noise-tolerant zeroing neural network (NTZNN) model with fixed-time convergence for solving the multi-linear system (1.1) with nonsingular \mathcal{M} -tensors. The NTZNN model can be regarded as a generalization of the extended ZNN model [41]. Furthermore, the NTZNN model achieves fixed-time convergence under ideal environments and various noise disturbances. Compared with existing models, including the CTNN model, the ZNN model, and the NSDTND model, the proposed NTZNN model has better convergence performance and retains noise tolerance. The main contributions of this paper are outlined as follows.

- 1) By introducing a novel nonlinear activation function, we propose an NTZNN model for solving multi-linear systems with nonsingular \mathcal{M} -tensors. This model can be viewed as an extension of the extended ZNN model [41].
- 2) Theoretical analyses demonstrate that the NTZNN model has fixed-time convergence regardless of the presence of noise. Unlike the ZNN model [41], whose convergence time depends on the initial state, the upper bound of the convergence time for the NTZNN model is independent of its initial state value. Furthermore, the NTZNN model shows superior convergence performance while maintaining noise tolerance.
- 3) Numerical experiments indicate that the NTZNN model achieves faster convergence and maintains stronger robustness compared with the CTNN model [40], the ZNN model [41], and the NSDTND model [42].

The rest of this paper is organized as follows: In Section 2, we introduce some basic definitions and technical lemmas, and briefly review the NSDTND, ZNN, and CTNN models. Section 3 proposes the NTZNN model for solving the multi-linear system (1.1) with nonsingular \mathcal{M} -tensors. Meanwhile, the fixed-time convergence of the NTZNN model with or without the presence of noise is theoretically established. In Section 4, we present some simulation experiments to validate the effectiveness and superiority of the proposed model. Finally, we make some conclusions to end this paper in Section 5.

2. Preliminaries

In this section, we recall some basic definitions and technical lemmas that will be used in subsequent proofs. Meanwhile, to motivate our approach, we briefly review some existing neural network approaches for solving multi-linear systems with nonsingular \mathcal{M} -tensors.

2.1. Definitions and Lemmas

We use $\mathbb{R}^{[m,n]}$ to denote the set of all m th-order n -dimensional real tensors. A tensor $\mathcal{A} \in \mathbb{R}^{[m,n]}$ is called a nonnegative tensor if all of its entries are nonnegative. The following definition of tensor eigenvalues was introduced independently by Qi [46] and Lim [47].

Definition 2.1. Let $\mathcal{A} \in \mathbb{R}^{[m,n]}$. If a nonzero complex vector $x = (x_1, x_2, \dots, x_n)^T$ and a complex

scalar λ satisfy

$$\mathcal{A}x^{m-1} = \lambda x^{[m-1]},$$

where $x^{[m-1]} = (x_1^{m-1}, x_2^{m-1}, \dots, x_n^{m-1})^T$, then λ is called an eigenvalue of \mathcal{A} and x is called the corresponding eigenvector.

The maximum modulus of the eigenvalues of \mathcal{A} is called the spectral radius of \mathcal{A} [48], denoted by $\rho(\mathcal{A})$. For a tensor $\mathcal{A} \in \mathbb{R}^{[m,n]}$, if there exists a nonnegative tensor \mathcal{B} and a real number $s \geq \rho(\mathcal{B})$ satisfying $\mathcal{A} = s\mathcal{I} - \mathcal{B}$, then \mathcal{A} is called an \mathcal{M} -tensor [1], where \mathcal{I} is an identity tensor whose entries $\delta_{i_1 i_2 \dots i_m}$ are defined as

$$\delta_{i_1 i_2 \dots i_m} = \begin{cases} 1, & \text{if } i_1 = i_2 = \dots = i_m, \\ 0, & \text{otherwise.} \end{cases}$$

Specifically, \mathcal{A} is called a nonsingular \mathcal{M} -tensor if $s > \rho(\mathcal{B})$.

In the ZNN model, the partial derivative of $\mathcal{A}x^{m-1}$ with respect to variable x plays a crucial role. However, the process of directly calculating this partial derivative is quite sophisticated, significantly increasing the complexity of model processing. To overcome this limitation, Han [7] proved that $\mathcal{A}x^{m-1} = \tilde{\mathcal{A}}x^{[m-1]}$, where $\tilde{\mathcal{A}}$ is a partially symmetric tensor whose entries are defined as

$$\tilde{a}_{i i_2 \dots i_m} = \frac{1}{(m-1)!} \sum_{\pi} a_{i_1 \pi(i_2 \dots i_m)},$$

in which the sum is taken over all the permutations $\pi(i_2 \dots i_m)$. Thus, the partial derivative of $\mathcal{A}x^{m-1}$ with respect to variable x is given by

$$\frac{\partial \mathcal{A}x^{m-1}}{\partial x} = (m-1)\tilde{\mathcal{A}}x^{m-2}, \quad (2.1)$$

where $\tilde{\mathcal{A}}x^{m-2}$ is an $n \times n$ matrix with the entries defined by

$$(\tilde{\mathcal{A}}x^{m-2})_{ij} = \sum_{i_3, \dots, i_m=1}^n \tilde{a}_{i j i_3 \dots i_m} x_{i_3 \dots i_m}, \quad i, j = 1, 2, \dots, n.$$

Additionally, Han [7] obtained that $\tilde{\mathcal{A}}$ is a nonsingular \mathcal{M} -tensor when \mathcal{A} is a nonsingular \mathcal{M} -tensor.

For the dynamic system

$$\dot{x}(t) = g(t, x(t)), \quad x(0) = x_0, \quad (2.2)$$

where $\dot{x}(t)$ denotes the time derivative of $x(t)$, $x(t) \in \mathbb{R}^n$, and $g : \mathbb{R}_+ \times \mathbb{R}^n \rightarrow \mathbb{R}^n$ is a nonlinear function. The following assumes that the origin is an equilibrium solution of the system (2.2).

Definition 2.2. [49] The origin of the system (2.2) is called global finite-time stability if it is globally asymptotically stable and there exists a settling-time function $T(x_0) : \mathbb{R}^n \rightarrow \mathbb{R}_+ \cup \{0\}$ such that any solution $x(t, x_0)$ of (2.2) reaches an equilibrium point at some finite time, i.e., the solution $x(t, x_0) = 0$ for every $t \geq T(x_0)$.

Definition 2.3. [49] The origin of the system (2.2) is said to be fixed-time stable if it is globally finite-time stable and the settling-time function $T(x_0)$ is bounded, i.e., $\exists T_{\max} > 0$ satisfying $T_{\max} \geq T(x_0), \forall x_0 \in \mathbb{R}^n$.

Lemma 2.1. [35] For the system (2.2), if there exists a continuous radially unbounded function $V : \mathbb{R}^n \rightarrow \mathbb{R}_+ \cup \{0\}$ such that

$$\dot{V}(x(t)) \leq -(\alpha V^\theta(x(t)) + \beta V^\varphi(x(t)))^k,$$

where $\alpha, \beta, \theta, \varphi, k > 0$, $k\theta < 1$, and $k\varphi > 1$, then the origin of the system (2.2) is fixed-time stable, i.e., there exists a constant

$$T_{\max} := \frac{1}{\alpha^k(1-k\theta)} + \frac{1}{\beta^k(k\varphi-1)}$$

satisfying $T(x_0) \leq T_{\max}, \forall x_0 \in \mathbb{R}^n$.

2.2. Existing neural network models

For solving the multi-linear system (1.1) with nonsingular \mathcal{M} -tensors, Liu et al. [42] proposed the following discrete-time neural dynamics model, called the NSDTND model:

$$x_{k+1} = x_k - \frac{1}{m-1}(\tilde{\mathcal{A}}_k x_k^{m-2})^{-1} \times \left(\theta_1(\mathcal{A}_k x_k^{m-1} - b_k) + \theta_2 \sum_{i=0}^k (\mathcal{A}_i x_i^{m-1} - b_i) + (\mathcal{A}_k - \mathcal{A}_{k-1})x_k^{m-1} - (b_k - b_{k-1}) \right), \quad (2.3)$$

where $\theta_1 = p\omega$, $\theta_2 = p^2\varsigma$, $\omega > 0$, $\varsigma > 0$, the sampling gap $p > 0$, and the parameters θ_1 and θ_2 satisfy $4\theta_2 < \theta_1^2$.

Wang et al. [41] presented the general zeroing neural network model as follows:

$$\dot{\varepsilon}(t) = -\xi \Psi(\varepsilon(t)), \quad (2.4)$$

where $\xi > 0$, $\varepsilon(t) = \mathcal{A}x(t)^{m-1} - b$ is called an error function, $x(t)$ is an unknown n -dimensional dynamic vector, $\dot{\varepsilon}(t)$ is the time derivative of $\varepsilon(t)$, $\varepsilon_i(t)$ denotes the i th component of $\varepsilon(t)$, and $\Psi(\cdot) : \mathbb{R}^n \rightarrow \mathbb{R}^n$ is an activation function array whose entries $\psi_i = \psi(\varepsilon_i(t))$ are monotonically increasing odd functions, which force the error $\varepsilon(t)$ to converge to zero.

Obviously, if $\Psi(\varepsilon(t))$ converges to the zero vector (i.e., an equilibrium point of the system (2.4)), then the error function $\varepsilon(t)$ converges to the zero vector, which implies that $x(t)$ converges to the theoretical solution x_* of (1.1). Due to the continuous differentiability of $\mathcal{A}x(t)^{m-1} - b$ with respect to $x(t)$, $\dot{\varepsilon}(t)$ can be rewritten as

$$\dot{\varepsilon}(t) = \frac{d\varepsilon(t)}{dt} = \frac{\partial \varepsilon(t)}{\partial x(t)} \frac{dx(t)}{dt} = \frac{\partial(\mathcal{A}x(t)^{m-1} - b)}{\partial x(t)} \frac{dx(t)}{dt}. \quad (2.5)$$

Combining (2.1), (2.4), and (2.5), we obtain the following implicitly defined dynamic system

$$\tilde{\mathcal{A}}x(t)^{m-2} \frac{dx(t)}{dt} = -\nu \Psi(\mathcal{A}x(t)^{m-1} - b), \quad (2.6)$$

where $\nu = \frac{\xi}{(m-1)}$. Note that if $\tilde{\mathcal{A}}x(t)^{m-2}$ is invertible, then it follows from (2.6) that

$$\dot{x}(t) = \frac{dx(t)}{dt} = -\nu(\tilde{\mathcal{A}}x(t)^{m-2})^{-1} \Psi(\mathcal{A}x(t)^{m-1} - b). \quad (2.7)$$

If $\tilde{\mathcal{A}}x_*^{m-2}$ is invertible, then the zeroing neural network model (2.6) converges to the solution x_* of (1.1) [41]. Specifically, for \mathcal{A} being a nonsingular \mathcal{M} -tensor and b being a positive vector, according to [1, Theorem 3.2], $\tilde{\mathcal{A}}x_*^{m-2}$ is invertible. Therefore, in this case, the zeroing neural network model (2.6) can solve (1.1).

According to (2.6), it can be seen that choosing different activation functions will yield different zeroing neural network models.

- If

$$\psi_i = \varepsilon_i(t), \quad (2.8)$$

then (2.6) is the continuous-time neural network (CTNN) model presented by Wang et al. [40].

- If

$$\psi_i = |\varepsilon_i(t)|^\theta \text{sign}(\varepsilon_i(t)), \quad (2.9)$$

where

$$\text{sign}(\varepsilon_i(t)) = \begin{cases} 1, & \text{if } \varepsilon_i(t) > 0, \\ 0, & \text{if } \varepsilon_i(t) = 0, \\ -1, & \text{if } \varepsilon_i(t) < 0, \end{cases}$$

then (2.6) is the simplified ZNN model given by Wang et al. [41].

- If

$$\psi_i = (k_1 |\varepsilon_i(t)|^\theta + k_2 |\varepsilon_i(t)|^\varphi) \text{sign}(\varepsilon_i(t)), \quad (2.10)$$

where $\theta \in (0, 1)$, $\varphi \in [1, +\infty)$, $k_1 > 0$, $k_2 > 0$, then (2.6) is the extended ZNN model proposed by Wang et al. [41].

- If

$$\psi_i(\varepsilon_i(t)) = \begin{cases} \Lambda_i(z), & \varepsilon_i(t) > z, \\ \Lambda_i(\varepsilon_i), & -\eta \leq \varepsilon_i(t) \leq \eta, \\ \Lambda_i(-z), & \varepsilon_i(t) < -z, \end{cases} \quad (2.11)$$

where $\Lambda_i(\cdot)$ is the simplified activation function (2.9), η and z are positive parameters satisfying $\eta \leq z$, then (2.6) is the piecewise ZNN model provided by Wang et al. [41]. As shown in [41], when $\eta = z$, the piecewise activation function (2.11) is continuous and exhibits the saturation property. Conversely, when $\eta < z$, the set of projections is nonconvex. Thus, in this case, (2.11) is a nonconvex activation function.

Wang et al. [41] pointed out that their proposed ZNN models have finite-time convergence, while the CTNN model does not converge in finite time because its activation function is linear. Hence, compared with the CTNN method, their models are more effective for solving the multi-linear system (1.1) with nonsingular \mathcal{M} -tensors. However, the convergence of these above-mentioned models cannot be guaranteed in the impact of noise disturbance that is inevitable and ubiquitous in practical life. Hence, we propose a noise-tolerant zeroing neural network model in the next section.

3. Proposed NTZNN model and theoretical analysis

As mentioned in previous parts, the CTNN model [40] and the ZNN models presented by Wang et al. [41] do not consider noise disturbances. In this section, we propose a fixed-time convergent ZNN model with noise-tolerance for solving the multi-linear system (1.1) with nonsingular \mathcal{M} -tensors.

For the zeroing neural network model (2.6), we propose a new activation function $\Psi^{nt}(\varepsilon(t))$ whose every entry is defined as

$$\Psi_i^{nt} = (k_1|\varepsilon_i(t)|^\theta + k_2|\varepsilon_i(t)|^\varphi)^k \text{sign}(\varepsilon_i(t)) + k_3\varepsilon_i(t) + k_4\text{sign}(\varepsilon_i(t)), \quad (3.1)$$

where the parameters satisfy $0 < k\theta < 1, k\varphi > 1, k_1, k_2 > 0, k_3, k_4 \geq 0$. It is easy to observe that (3.1) reduces to (2.10) given by Wang et al. [41] when $k = 1, k_3 = k_4 = 0$. Thus, combining (2.4) with (3.1), we obtain the following noise-tolerant ZNN model

$$\dot{\varepsilon}(t) = -\xi\Psi^{nt}(\varepsilon(t)), \quad (3.2)$$

where $\xi > 0, \varepsilon(t) = \mathcal{A}x(t)^{m-1} - b$. It can be reformulated as

$$\tilde{\mathcal{A}}x(t)^{m-2} \frac{dx(t)}{dt} = -\nu\Psi^{nt}(\varepsilon(t)),$$

in which $\nu = \frac{\xi}{m-1}$. For simplicity, we call it the NTZNN model. Obviously, the NTZNN model is a generalization of the extended ZNN model (2.10) proposed by Wang et al. [41]. The following will prove that the NTZNN model (3.2) achieves fixed-time convergence and exhibits strong robustness against both the time-varying bounded nonvanishing/vanishing noise.

3.1. Convergence analysis of NTZNN model in an ideal situation

Let x_* be a solution to (1.1) satisfying that $\tilde{\mathcal{A}}x_*^{m-2}$ is nonsingular. We define the neighborhood of x_* as $\Omega(x_*, \delta) = \{x \in \mathbb{R}^n \mid \|x - x_*\|_2 \leq \delta\}$ for some $\delta > 0$ such that $\tilde{\mathcal{A}}x^{m-2}$ is nonsingular for all $x \in \Omega(x_*, \delta)$. The following theorem shows that the NTZNN model (3.2) without noise disturbances achieves fixed-time convergence.

Theorem 3.1. *Suppose that x_* is a solution to the multi-linear system (1.1). If $\tilde{\mathcal{A}}x_*^{m-2}$ is nonsingular, then the neural state solution $x(t)$ of the NTZNN model (3.2) converges to the theoretical solution x_* for any initial state $x(0) \in \Omega(x_*, \delta)$ with the settling-time function bounded by*

$$T_{max}^{nt} = \frac{1}{\xi k_1^k (1 - k\theta)} + \frac{1}{\xi k_2^k (k\varphi - 1)}, \quad (3.3)$$

where the parameters $k_1, k_2, k, \theta, \varphi$ are given by (3.1) and $\xi > 0$.

Proof. According to the NTZNN model (3.2), we only need to prove that each of its subsystem

$$\dot{\varepsilon}_i(t) = -\xi\Psi_i^{nt} \quad (3.4)$$

is fixed-time convergent, where $\varepsilon_i(t)$ represents the i th element of error function $\varepsilon(t) = \mathcal{A}x(t)^{m-1} - b$.

Define a Lyapunov function $u_i(t) = |\varepsilon_i(t)| \geq 0$. According to the derivative of $u_i(t)$ and (3.4), we have

$$\begin{aligned} \dot{u}_i(t) &= \dot{\varepsilon}_i(t) \operatorname{sign}(\varepsilon_i(t)) \\ &= -\xi[(k_1|\varepsilon_i(t)|^\theta + k_2|\varepsilon_i(t)|^\varphi)^k \operatorname{sign}(\varepsilon_i(t)) + k_3\varepsilon_i(t) + k_4\operatorname{sign}(\varepsilon_i(t))]\operatorname{sign}(\varepsilon_i(t)) \\ &= -\xi[(k_1|\varepsilon_i(t)|^\theta + k_2|\varepsilon_i(t)|^\varphi)^k + k_3|\varepsilon_i(t)| + k_4] \\ &\leq -\xi(k_1|\varepsilon_i(t)|^\theta + k_2|\varepsilon_i(t)|^\varphi)^k \\ &= -\xi(k_1u_i(t)^\theta + k_2u_i(t)^\varphi)^k \\ &\leq 0, \end{aligned}$$

which implies that $\varepsilon_i(t)$ converges globally and asymptotically to zero over time for all i . This shows that the error vector $\varepsilon(t)$ converges globally and asymptotically to zero over time. In addition, since $k, k_1, k_2, \theta, \varphi$ satisfy the requirements in (3.1), it follows from Lemma 2.1 that the convergence time $T_i(x(0))$ of the $\varepsilon_i(t)$ is

$$T_i(x(0)) \leq \frac{1}{\xi k_1^k (1 - k\theta)} + \frac{1}{\xi k_2^k (k\varphi - 1)} = T_{\max}^{nt}.$$

Therefore, the model (3.2) is fixed-time convergent. Thus the proof is completed. \square

Theorem 3.1 indicates that the NTZNN model (3.2) is fixed-time convergent as long as a solution x_* of the multi-linear system (1.1) satisfies that $\tilde{\mathcal{A}}x_*^{m-2}$ is nonsingular. Hence, according to [1, Theorem 3.2], the NTZNN model can be effectively applied to solve the multi-linear system (1.1) with \mathcal{A} being a nonsingular \mathcal{M} -tensor and b being a positive vector.

3.2. Convergence analysis of NTZNN model with the influence of some noise

In practical life, noise disturbances are inevitable and ubiquitous, such as external disturbance, model uncertainty, or computational error. Therefore, it is essential to analyze the impact of noise on the solution of the proposed NTZNN model (3.2) to ensure robustness and reliability. In this section, we investigate the convergence of the NTZNN model with time-varying bounded vanishing/nonvanishing noise. Supposing $y(t)$ represents time-varying noise with a vector value, the noise-perturbed NTZNN model is formulated as follows:

$$\dot{\varepsilon}(t) = -\xi\Psi^m(\varepsilon(t)) + y(t). \quad (3.5)$$

In the NTZNN model (3.5), the noise term $y(t)$ represents external disturbances or perturbations that affect the dynamic system during its operation. For example, the measurement noise caused by inaccurate sensors during data collection for the multilinear system (1.1) usually introduces time-varying disturbances. Additionally, finite-precision computation in digital hardware causes round-off errors during tensor operations, leading to nonvanishing noise.

The following theorem indicates the convergence of the model (3.5) with bounded noise.

Theorem 3.2. *Let x_* be a solution to the multi-linear system (1.1). Assume that $\tilde{\mathcal{A}}x_*^{m-2}$ is nonsingular and the entries of the noise $y(t)$ satisfy*

$$|y_i(t)| \leq \gamma|\varepsilon_i(t)| + \tau, \quad i = 1, 2, \dots, n. \quad (3.6)$$

If $\gamma \in (0, \xi k_3)$ and $\tau \in (0, \xi k_4)$, where ξ, k_3 , and k_4 are given by (3.5), then the state solution $x(t)$ of the model (3.5) converges to the theoretical solution x_ for all initial states $x(0) \in \Omega(x_*, \delta)$ with the settling-time function bounded by T_{\max}^{nt} .*

Proof. Define a Lyapunov function $u_i(t) = |\varepsilon_i(t)|^2 \geq 0$; it follows from the time derivative of $u_i(t)$ and model (3.5) that

$$\begin{aligned}\dot{u}_i(t) &= 2\varepsilon_i(t)\dot{\varepsilon}_i(t) \\ &= -2\xi[(k_1|\varepsilon_i(t)|^\theta + k_2|\varepsilon_i(t)|^\varphi)^k|\varepsilon_i(t)| + k_3\varepsilon_i^2(t) + k_4|\varepsilon_i(t)|] + 2\varepsilon_i(t)y_i(t) \\ &\leq -2\xi[(k_1|\varepsilon_i(t)|^{\theta+\frac{1}{k}} + k_2|\varepsilon_i(t)|^{\varphi+\frac{1}{k}})^k] + 2(\gamma - \xi k_3)\varepsilon_i^2(t) + 2(\tau - \xi k_4)|\varepsilon_i(t)| \\ &\leq -2\xi(k_1|\varepsilon_i(t)|^{\theta+\frac{1}{k}} + k_2|\varepsilon_i(t)|^{\varphi+\frac{1}{k}})^k \\ &= -2\xi(k_1u_i(t)^{\frac{(k\theta+1)}{2k}} + k_2u_i(t)^{\frac{(k\varphi+1)}{2k}})^k \\ &\leq 0.\end{aligned}$$

Hence, it follows from the Lyapunov theory that the error $\varepsilon_i(t)$ globally asymptotically converges to zero with time for all i , which implies that the error vector $\varepsilon(t)$ globally asymptotically converges to zero with time. Note that the parameters k, θ, φ satisfy $k\frac{(k\theta+1)}{2k} < 1$ and $k\frac{(k\varphi+1)}{2k} > 1$; thus according to Lemma 2.1, we obtain the fixed-time of the i th entry convergence of the vector $\varepsilon(t)$ is

$$\begin{aligned}&\frac{1}{2\xi k_1^k(1 - \frac{k\theta+1}{2})} + \frac{1}{2\xi k_2^k(\frac{k\varphi+1}{2} - 1)} \\ &= \frac{1}{\xi k_1^k(1 - k\theta)} + \frac{1}{\xi k_2^k(k\varphi - 1)} \\ &= T_{max}^{nt}.\end{aligned}$$

This indicates that the error vector $\varepsilon(t)$ converges globally and asymptotically to zero in the fixed-time T_{max}^{nt} . \square

According to Theorem 3.2, if $\gamma = 0$, the inequality (3.6) reduces to $|y_i(t)| \leq \tau$, which represents time-varying bounded nonvanishing noise. This indicates that the model (3.5) is convergent under the time-varying bounded nonvanishing noise as long as $\tau \in (0, \xi k_4)$. Additionally, if $\tau = 0$, then the inequality (3.6) becomes $|y_i(t)| \leq \gamma|\varepsilon_i(t)|$, corresponding to time-varying bounded vanishing noise. This implies that the model (3.5) is convergent under time-varying bounded vanishing noise as long as $\gamma \in (0, \xi k_3)$.

4. Numerical examples

In this section, some numerical examples are presented to illustrate the effectiveness and efficiency of our proposed NTZNN model (3.2). To demonstrate the superiority of the NTZNN model, we compare it with the NSDTND model [42], the CTNN method [40], and three zeroing neural dynamic models developed by Wang et al. [41], including the simplified zeroing neural dynamic model (2.9), the extended zeroing neural dynamic model (2.10), and the piecewise zeroing neural dynamic model (2.11), which are referred to as the simplified, extended, and piecewise models for short. All codes were written in the software MATLAB R2017, and all tests were performed on a portable computer equipped with a 3.20 GHz Intel Core i7-8700U and 8.00 GB RAM memory. In addition, we used the MATLAB routine ode45 for solving the ordinary differential equation. To ensure superior performance for each example, the parameters are consistently set as follows: $k_1 =$

$3, k_2 = 1, k_3 = k_4 = 3, \theta = \frac{1}{15}, \varphi = 1.01$ in Example 4.1; $k_1 = 1, k_2 = 1, k_3 = 1, k_4 = 1, \theta = \frac{1}{6}, \varphi = 1.01$ in Examples 4.2 and 4.3; $k_1 = k_4 = 3, k_2 = k_3 = 2, \theta = \frac{1}{10}, \varphi = 1.2$ in Example 4.4.

4.1. Numerical results for solving multi-linear systems with nonsingular \mathcal{M} -tensors

Example 4.1. We construct a nonsingular \mathcal{M} -tensor $\mathcal{A} = s\mathbf{I} - \mathcal{B}$, where $\mathcal{B} \in \mathbb{R}^{[m,n]}$ is a nonnegative tensor whose every entry is randomly generated from the standard uniform distribution on $(0, 1)$, the scalar $s = (1 + \varpi) \max_{i=1,2,\dots,n} (\mathcal{B}\mathbf{I}^{m-1})_i$, $\varpi > 0$, $\mathbf{I} = [1, 1, \dots, 1]^T$.

In this experiment, we set $\varpi = 0.05$, $b = [1, 2, \dots, n]^T$, $\xi = 1$, and the initial state $x(0)$ of all models is chosen as the vector $\text{rand}(n, 1)$ in MATLAB. The parameter k in the NTZNN model is set to $k = 1.5$, and the parameters for NSDTND models are set to $p = 0.1, \theta_1 = 0.3, \theta_2 = 0.01$. Figure 1 plots the variation of the residual error $\|\varepsilon(t)\|_2$ of different models over time t under a noiseless situation, where $\|\cdot\|_2$ denotes the Euclidean norm. It follows from Figure 1 that the NTZNN model has faster convergence speed and higher accuracy compared to the NSDTND model, the CTNN model, the simplified ZNN model, the extended ZNN model, and the piecewise ZNN model. This means that the proposed NTZNN model can more effectively solve the multi-linear system (1.1) with nonsingular \mathcal{M} -tensors.

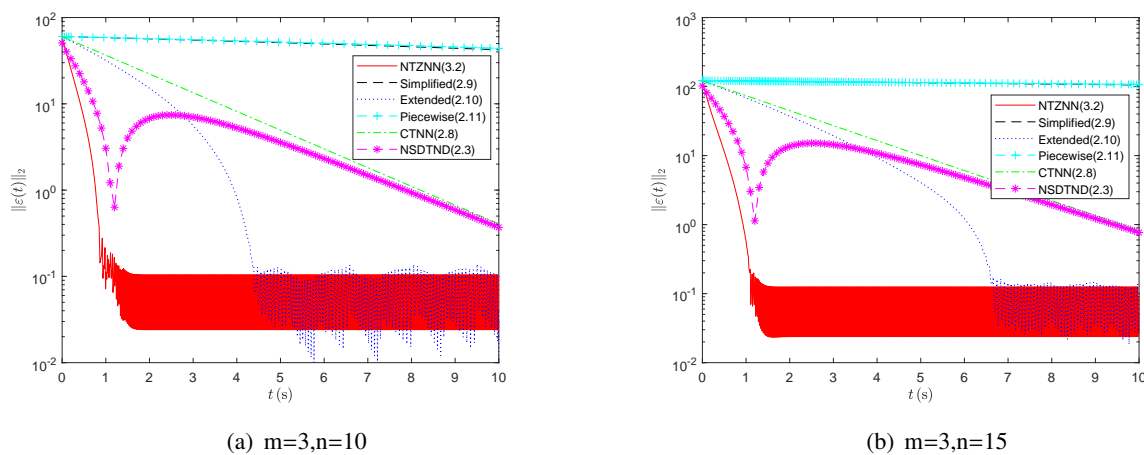


Figure 1. The variation of residual error $\|\varepsilon(t)\|_2$ generated by the NTZNN model (3.2), the CTNN model (2.8), the Simplified model (2.9), the Extended model (2.10), the Piecewise model (2.11), and the NSDTND model (2.3) with different dimensions and orders.

Figure 2 depicts that when $m = 3, n = 10$, the variation of the residual error $\|\varepsilon(t)\|_2$ over time t for different models under two types of noise situations, i.e., the time-varying bounded vanishing noise $y_i(t) = 0.4\varepsilon_i(t)$ and the time-varying bounded nonvanishing noise $y_i(t) = 0.6$. As shown in Figure 2, the NTZNN model exhibits superior convergence performance in the presence of noise. Compared with other models, it not only converges faster but also has greater stability, thereby effectively maintaining its noise resistance.

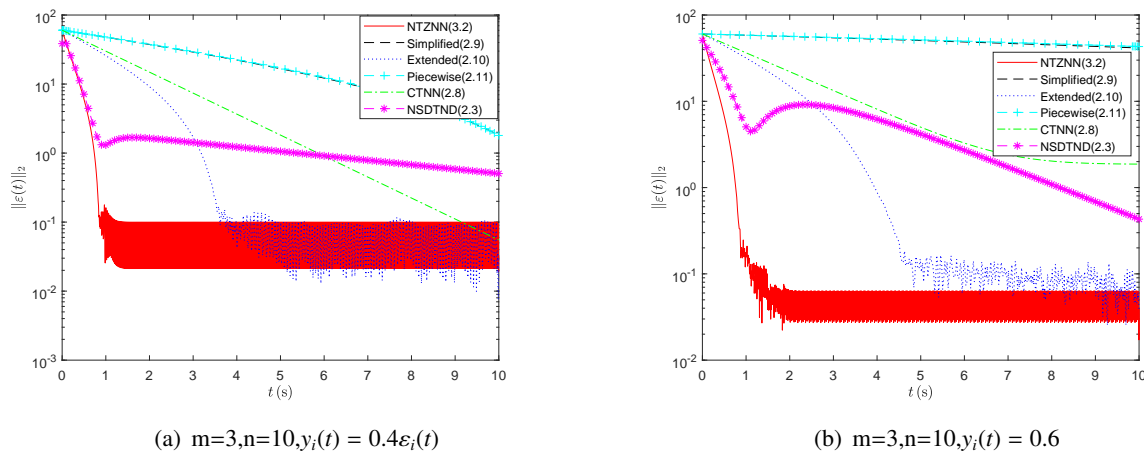


Figure 2. The variation of residual error $\|\varepsilon(t)\|_2$ generated by the NTZNN model (3.2), the CTNN model (2.8), the Simplified model (2.9), the Extended model (2.10), the Piecewise model (2.11), and the NSDTND model (2.3) under different noises, i.e., (a) with the time-varying bound vanishing noise $y_i(t) = 0.4\varepsilon_i(t)$; (b) with the time-varying bound nonvanishing noise $y_i(t) = 0.6$.

Figure 3 plots the variation of the residual error $\|\varepsilon(t)\|_2$ over time t for the NTZNN model when $m = 3, n = 10$, under different initial values, different values of k , and different values of φ . Figure 3(a) shows the NTZNN model eventually all converges to the same order of magnitude (around 10^{-2}) within the theoretically predicted fixed time $T_{max}^{nt} \approx 2.156(s)$ for different initial values, indicating that the convergence of the model is independent of the initial values and achieves the fixed-time convergence. It follows from Figure 3(b) that the convergence speed of the NTZNN model is different as k varies. Figure 3(c) reveals that the convergence speed and residual error of the NTZNN model are affected by different values of φ .

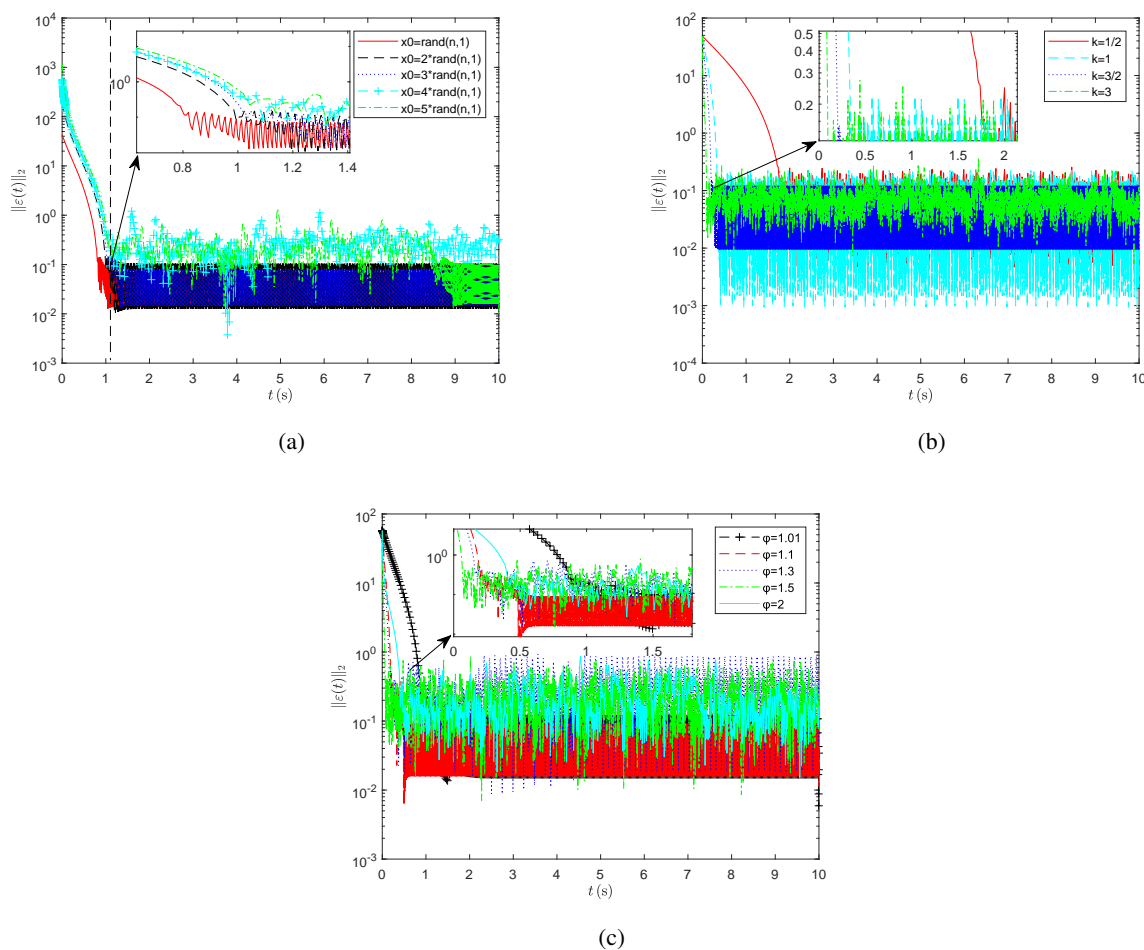


Figure 3. The variation of residual error $\|\varepsilon(t)\|_2$ generated by the NTZNN model (3.2) under different parameter settings, i.e., (a) different initial values x_0 ; (b) different values k ; (c) different values φ .

Example 4.2. Consider a nonnegative tensor $\mathcal{B} \in \mathcal{R}^{[m,n]}$ with its entries

$$b_{i_1 \dots i_m} = |\sin(i_1 + i_2 + \dots + i_m)|,$$

and let $\mathcal{A} = s\mathcal{I} - \mathcal{B}$, where $s > \max_{1 \leq i \leq m} \sum_{i_2, \dots, i_m=1}^n b_{ii_2 \dots i_m}$. Then the tensor \mathcal{A} is a nonsingular \mathcal{M} -tensor according to [1, Lemma 5.2].

In this experiment, we take $b = [100, 200, \dots, 100n]^T$, $\xi = 10000$, and initialize the state of all models $x(0) = [1, 1, \dots, 1]^T$. The parameter k in the NTZNN model is set to $k = 1.5$. Figure 4 depicts the evolution of the residual error $\|\varepsilon(t)\|_2$ over time t for different models with differing values of m and n under a noiseless situation. Figure 5 plots the evolution of the residual error $\|\varepsilon(t)\|_2$ over time t for different models with $m = 4$ and $n = 20$ under two types of noise situations, i.e., the time-varying bounded vanishing noise $y_i(t) = 0.4\varepsilon_i(t)$ and the time-varying bound nonvanishing noise $y_i(t) = 0.6$. Here, we take $s = 7000, 30000, 60000, 6200$ respectively for different $(m, n) = (3, 100), (3, 200), (3, 300), (4, 20)$. As shown in Figures 4 and 5, the NTZNN model has significantly

faster convergence than the CTNN model [40] as well as the simplified, extended, and piecewise ZNN models [41], regardless of the presence of some noise. Moreover, its residual error remains consistently lower than that of other models. These results indicate that the NTZNN model has superior convergence speed and enhanced robustness compared to other models.

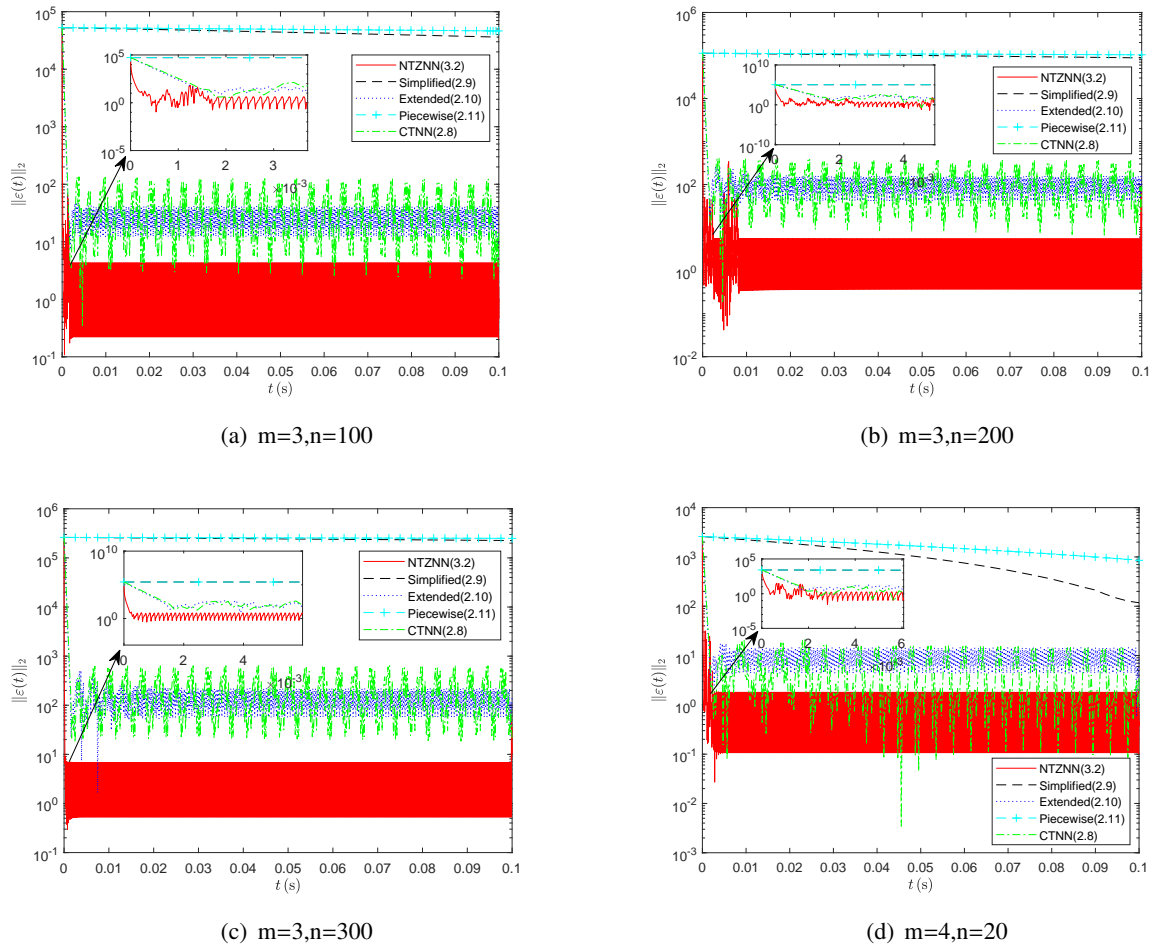


Figure 4. The variation of residual error $\|\varepsilon(t)\|_2$ generated by the NTZNN model (3.2), the CTNN model (2.8), the Simplified model (2.9), the Extended model (2.10), and the Piecewise model (2.11) with different dimensions and orders.

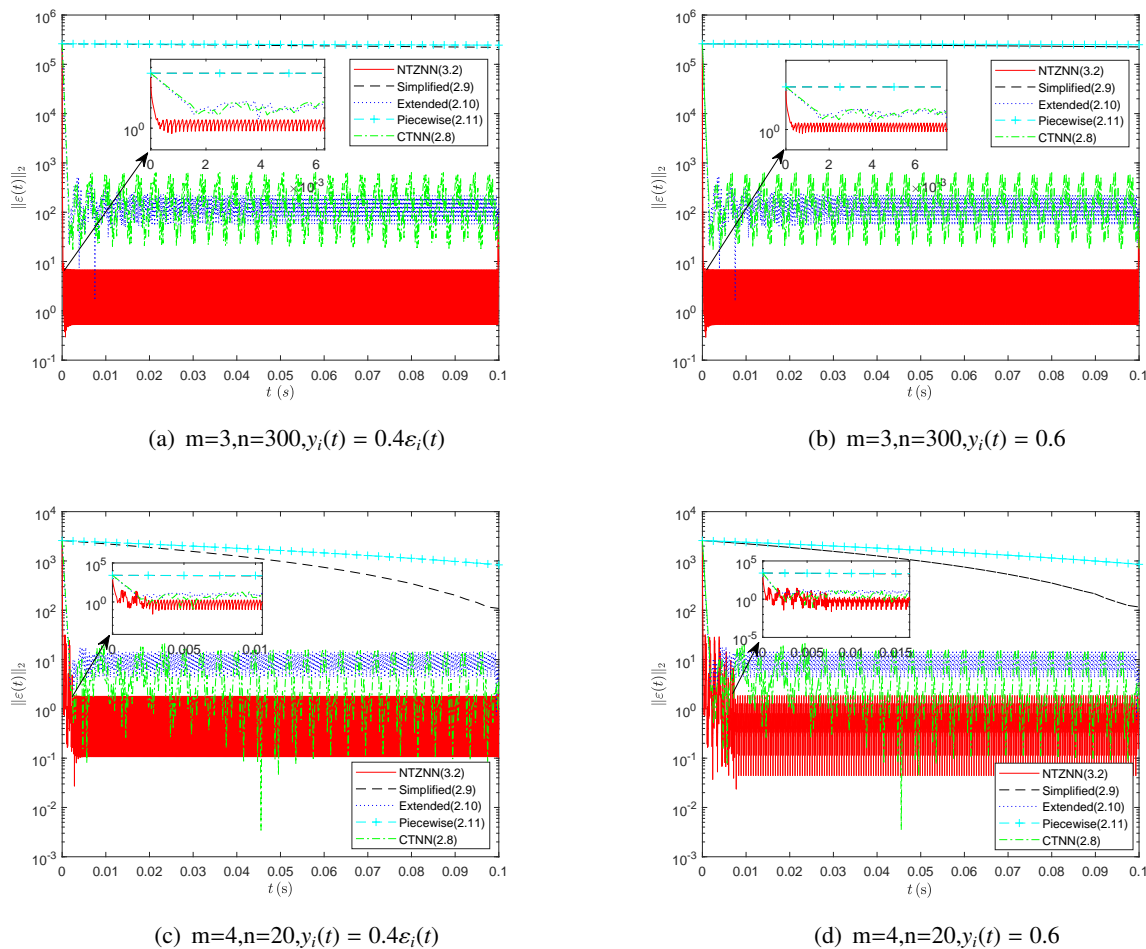


Figure 5. The variation of residual error $\|\epsilon(t)\|_2$ generated by the NTZNN model (3.2), the CTNN model (2.8), the simplified model (2.9), the extended model (2.10), and the piecewise model (2.11) under different noises, i.e., with the time-varying bounded vanishing noise $y_i(t) = 0.4\epsilon_i(t)$ in (a) and (c); with the time-varying bounded nonvanishing noise $y_i(t) = 0.6$ in (b) and (d).

4.2. Numerical results for application to differential equations

In this subsection, the NTZNN model is applied to solve two numerical examples driven from partial differential equations. The following example is given by Ding et al. [1].

Example 4.3. Consider the differential equation

$$\frac{d^2 x(t)}{dt^2} = -\frac{GM}{x(t)^2} \text{ in } (0, 1)$$

with Dirichlet boundary conditions $x(0) = c_0, x(1) = c_1$. Here $M \approx 5.98 \times 10^{24} \text{ kg}$ is the mass of the Earth and $G \approx 6.67 \times 10^{-11} \text{ Nm}^2/\text{kg}^2$ is the gravitational constant. If $c_0 > 0$ and $c_1 > 0$, this equation can be used to describe the motion of particles under the action of gravity.

As shown in [1], after the discretization of the above differential equation, we obtain the following polynomial equation system

$$\begin{cases} x_1^3 = c_0^3, \\ 2x_i^3 - x_i^2 x_{i-1} - x^2 x_{i+1} = \frac{GM}{(n-1)^2}, \quad i = 2, 3, \dots, n-1, \\ x_n^3 = c_1^3. \end{cases}$$

It can be rewritten as a multi-linear system $\mathcal{A}x(t)^3 = b$, where \mathcal{A} is a 4-order n -dimensional tensor whose elements are given by

$$\begin{cases} a_{1111} = a_{nnnn} = 1, \\ a_{iiii} = 2, \quad i = 2, 3, \dots, n-1, \\ a_{i(i-1)ii} = a_{ii(i-1)i} = a_{iii(i-1)} = -\frac{1}{3}, \\ a_{i(i+1)ii} = a_{ii(i+1)i} = a_{iii(i+1)} = -\frac{1}{3}, \end{cases}$$

and the right-hand side b is a positive vector with entries

$$\begin{cases} b_1 = c_0^3, \\ b_i = \frac{GM}{(n-1)^2}, \quad i = 2, 3, \dots, n-1, \\ b_n = c_1^3. \end{cases}$$

It is straightforward to verify that \mathcal{A} is a nonsingular \mathcal{M} -tensor. Consequently, this problem can be solved by using the NTZNN model, the CTNN model [40], and the simplified/extended/piecewise ZNN model [41]. In this experiment, we take $n = 10$, $\xi = 30$, and the initial state of all models $x_0 = [6370, 6370, \dots, 6370]^T$. Additionally, we set the parameter $k = 1.1$ in the NTZNN model. Figure 6 describes the evolution of the residual error $\|\varepsilon(t)\|_2$ over time t for different models in the non-noise environment (i.e., $y_i(t) = 0$), the presence of time-varying bounded vanishing noise $y_i(t) = 0.4\varepsilon_i(t)$, the presence of time-varying bounded nonvanishing noise $y_i(t) = 10$, respectively. From Figure 6, it can be seen that the NTZNN model achieves faster convergence than other methods regardless of the presence of some noises. Notably, under the influence of noise, the convergence of the NTZNN model still remains stable. These results indicate that the NTZNN model (3.2) maintains noise tolerance and has better performance for solving the tensor Eq (1.1) with nonsingular \mathcal{M} -tensors.

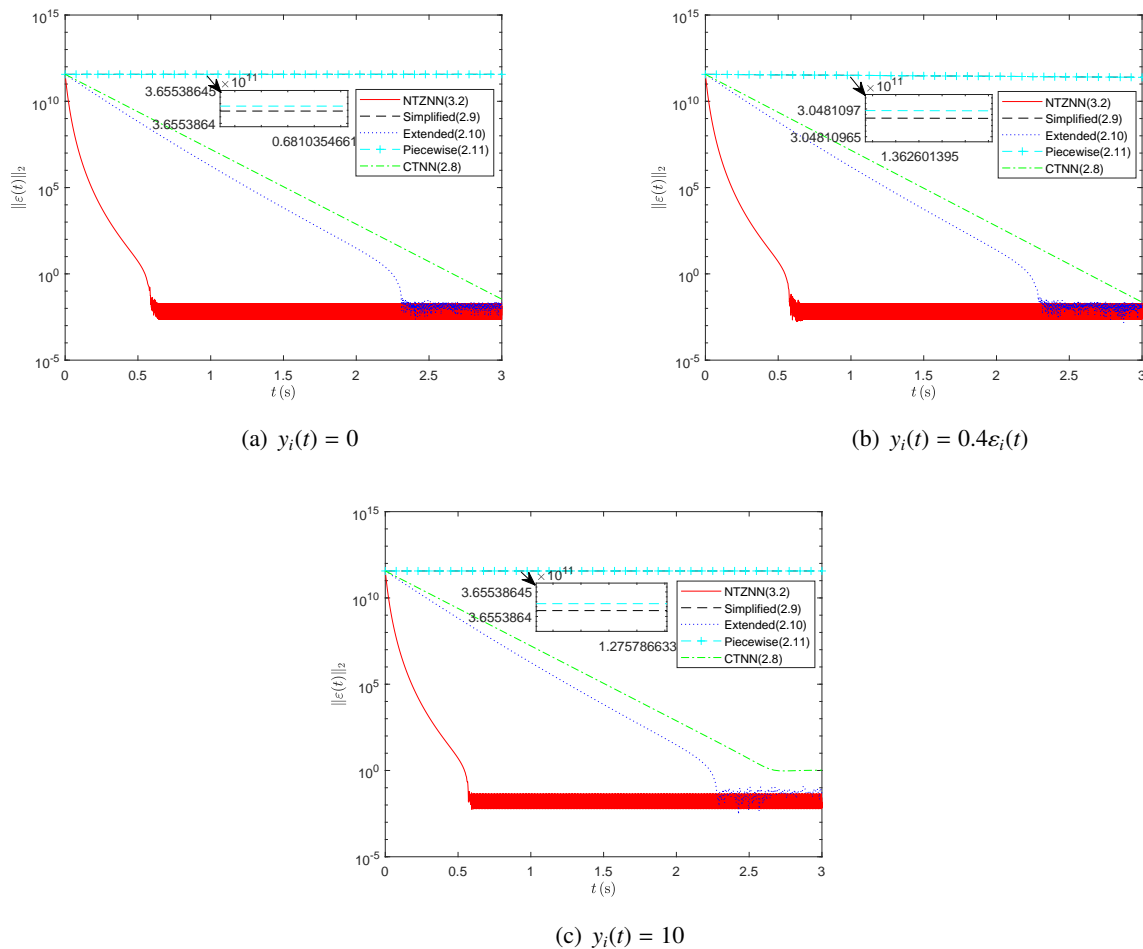


Figure 6. The variation of residual error $\|\varepsilon(t)\|_2$ generated by the NTZNN model (3.2), the CTNN model (2.8), the simplified model (2.9), the extended model (2.10), and the piecewise model (2.11) under different noises, i.e., (a) in the non-noise environment, i.e., $y_i(t) = 0$; (b) with the time-varying bounded vanishing noise $y_i(t) = 0.4\varepsilon_i(t)$; (c) with the time-varying bounded nonvanishing noise $y_i(t) = 10$.

Example 4.4. [40] Consider the numerical solution of the differential equation

$$\begin{cases} -\max_{(\kappa, \mathcal{K}) \in (\Lambda, \mathfrak{K})} L^\kappa U - \eta U - \frac{1}{2} \alpha \kappa^2 U + \beta \kappa = 0, & \text{on } \Omega, \\ U = g, & \text{on } \partial(\Omega), \end{cases} \quad (4.1)$$

where $L^\kappa U(x) = \frac{1}{2} \sigma(x, \kappa)^2 U''(x) + u(x, \kappa) U'(x)$, $\Omega = (0, 1)$, $\Lambda = [0, \infty)$ and \mathfrak{K} is a compact metric space. The differential Eq (4.1) is a Hamilton–Jacobi–Bellman (HJB) equation arising in optimal stochastic control problems.

As shown in [4, 40], using the strategy of “optimize and discretize” to discretize (4.1), we obtain a 3rd-order Bellman equation

$$\min_{\kappa \in \mathfrak{K}_{\Delta x}^{N+1}} \{\mathcal{A}(\kappa)u^2 = b\}, \quad (4.2)$$

where $u = (u_0, \dots, u_N)^T$ with $u_i \approx U(i\Delta x)$ for $i = 0, \dots, N$, $\kappa = (\kappa_0, \dots, \kappa_N)^T \in \mathfrak{N}_{\Delta x}^{N+1}$ with $\kappa_i \in \mathfrak{N}_{\Delta x}$, $\Delta x = \frac{1}{N}$, and $\mathcal{A}(\kappa) = (a_{ijk}(\kappa))$ is a 3-order $N + 1$ -dimensional tensor with its nonzero entries defined by

$$\begin{cases} a_{i,i-1,i}(\kappa) = a_{i,i,i-1}(\kappa), & 0 < i < N, \\ 2a_{i,i,i-1}(\kappa) = -\frac{1}{2}\sigma_i(\kappa_i)^2 \frac{1}{(\Delta x)^2} + u_i(\kappa_i) \frac{1}{\Delta x} \mathbf{1}_{(-\infty,0)}(u_i(\kappa_i)), & 0 < i < N, \\ a_{i,i,i}(\kappa) = \frac{1}{2}\sigma_i(\kappa_i)^2 \frac{2}{(\Delta x)^2} + |u_i(\kappa_i)| \frac{1}{\Delta x} + \eta_i, & 0 < i < N, \\ 2a_{i,i,i+1}(\kappa) = -\frac{1}{2}\sigma_i(\kappa_i)^2 \frac{1}{(\Delta x)^2} - u_i(\kappa_i) \frac{1}{\Delta x} \mathbf{1}_{(0,+\infty)}(u_i(\kappa_i)), & 0 < i < N, \\ a_{i,i+1,i}(\kappa) = a_{i,i,i+1}(\kappa), & 0 < i < N, \\ a_{i,i,i}(\kappa) = 1, & i = 0, N, \end{cases}$$

where $\mathbf{1}_{(-\infty,0)}$ denotes an indicator function over the set $(-\infty, 0)$, $\eta_i = \eta(i\Delta x)$, $\sigma_i(\kappa_i) = \sigma(i\Delta x, \kappa_i)$, $u_i(\kappa_i) = u(i\Delta x, \kappa_i)$. The vector $b = (b_0, \dots, b_N)^T$ is given by

$$b_i = \begin{cases} \frac{1}{2} \frac{\beta_i^2}{\alpha_i}, & 0 < i < N, \\ g_i^2, & i = 0, N. \end{cases}$$

where $\alpha_i = \alpha(i\Delta x)$, $\beta_i = \beta(i\Delta x)$, $g_i = g(i\Delta x)$.

In this experiment, let

$$\sigma(x, \kappa_i) = 0.02, \quad \alpha(x) = 2 - x, \quad \eta(x) = 0.04, \quad u(x, \kappa_i) = 0.04\kappa_i, \quad \beta(x) = 1 + x, \quad g(x) = 1,$$

where $\kappa_i = \{-1, 1\}$, $\mathfrak{N}_{\Delta x} = \mathfrak{N}$. According to the discussion in [4], the tensor $\mathcal{A}(\kappa)$ is a nonsingular \mathcal{M} -tensors, and thus this equation $\mathcal{A}(\kappa)u^2 = b$ has a positive solution [1]. We utilize the NTZNN model, the CTNN model [40], and the simplified/extended/piecewise ZNN model [41] to solve this equation. Here, we take $N = 10$, $\xi = 1 \times 10^4$, and the initial state of all models $u_0 = \text{rand}(N + 1, 1)$ in MATLAB.

Figure 7 depicts the evolution of the residual error $\|\varepsilon(t)\|_2$ over time t for different models in both ideal environments (i.e., $y_i(t) = 0$) and noisy environments (including the time-varying bounded vanishing noise $y_i(t) = 0.4\varepsilon_i(t)$ and the time-varying bounded nonvanishing noise $y_i(t) = 0.6$), and shows the variation of the state solution $U(t)$ over time t for the NTZNN model in ideal environments (i.e., $y_i(t) = 0$). It can be observed from Figure 7 that regardless of the presence of noise, the NTZNN model (3.2) converges faster than other methods, indicating that the NTZNN model (3.2) has superior performance in solving the multi-linear system (1.1) with non-singular \mathcal{M} -tensors.

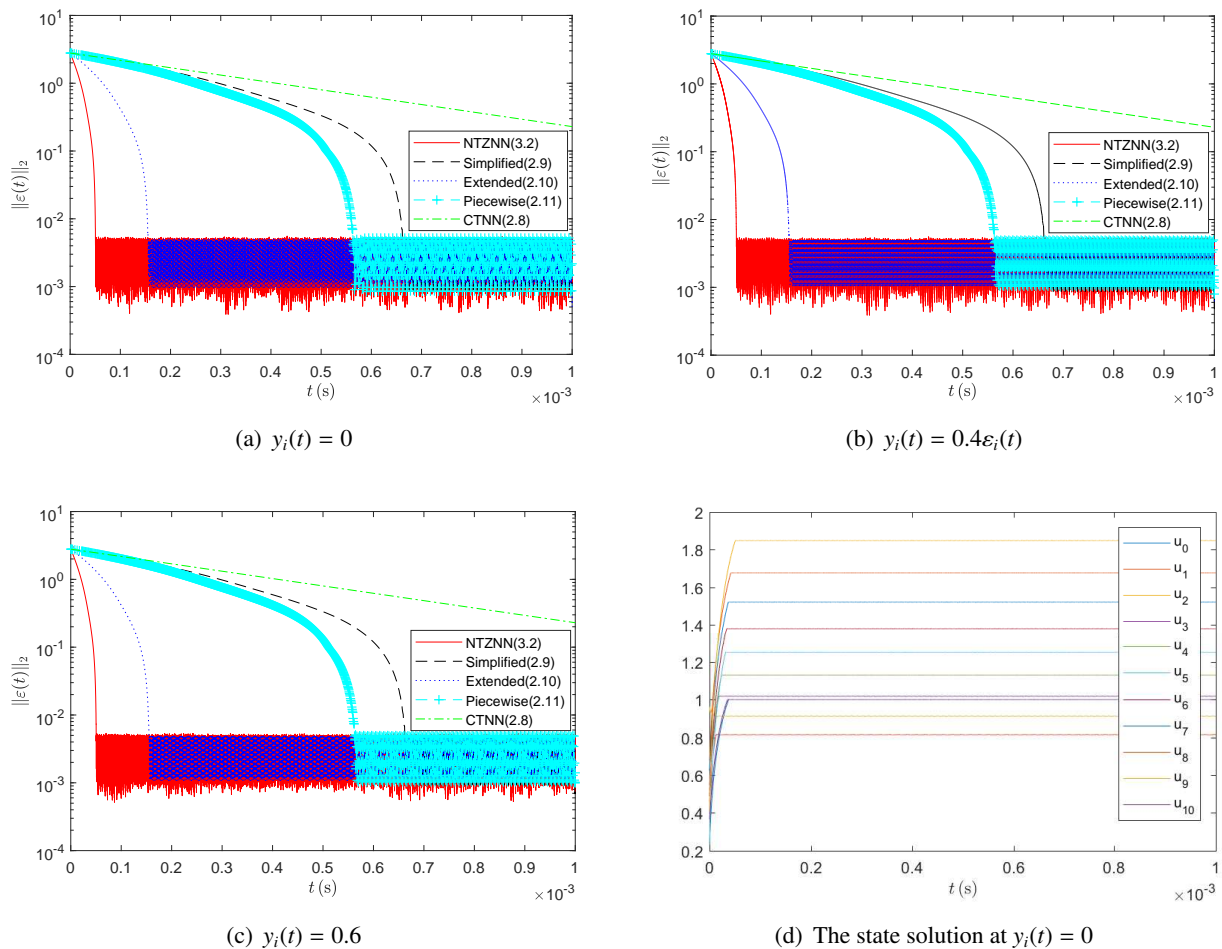


Figure 7. The variation of residual error $\|\varepsilon(t)\|_2$ generated by the NTZNN model (3.2), the CTNN model (2.8), the Simplified model (2.9), the Extended model (2.10), and the Piecewise model (2.11) under different noises, i.e., (a) in the non-noise environment; (b) with the time-varying bounded vanishing noise $y_i(t) = 0.4\varepsilon_i(t)$; (c) with the time-varying bounded nonvanishing noise $y_i(t) = 0.6$; (d) the evolution of the state solution $U(t)$ over time t for the NTZNN model in ideal environments (i.e., $y_i(t) = 0$).

5. Conclusions

In this paper, we propose the NTZNN model based on a novel nonlinear activation function to effectively solve the multi-linear system with nonsingular \mathcal{M} -tensors. This model can be regarded as a generalization of the extended ZNN model given in [41]. The theoretical analysis demonstrates that the NTZNN model has fixed-time convergence in both the ideal environment and the presence of the time-varying bounded vanishing/nonvanishing noise. Compared with existing approaches, including the NSDTND model [42], the CTNN model [40], and the ZNN models [41], the proposed NTZNN model not only achieves fixed convergence time but also maintains noise-tolerant performance. Numerical

experiments are performed to further verify our theoretical results and show that the proposed NTZNN model achieves significantly faster convergence and exhibits stronger robustness compared with the existing NSDTND, CTNN, and ZNN models. Nevertheless, the proposed model still has limited ability in suppressing unbounded noise or unknown noise. Therefore, in the future, we will design new ZNN models to handle other types of noise. Additionally, we will also consider some ZNN models for solving time-varying multilinear systems.

Author contributions

Ruijuan Zhao: Conceptualization, methodology, supervision, writing-review & editing; Mengyao Li: Software, formal analysis, writing-original draft, visualization; Tingjia Liu: Software; Shuxin Miao: Supervision. All authors have read and approved the final version of the manuscript for publication.

Use of Generative-AI tools declaration

The authors declare they have not used Artificial Intelligence (AI) tools in the creation of this article.

Acknowledgements

The work is supported by National Natural Science Foundation of China (Nos.12201267, 12361081), Science and Technology Project of Gansu Province (No.22JR5RA559), Education technology innovation project of Gansu Province (No.2025CXZX-874) and Innovation Foundation of Education Department of Gansu Province (No.2024A-125).

Conflict of interest

The authors declare that they have no conflict of interest.

References

1. W. Ding, Y. Wei, Solving multi-linear systems with \mathcal{M} -tensors, *J. Sci. Comput.*, **68** (2016), 689–715. <https://doi.org/10.1007/s10915-015-0156-7>
2. X. Li, M. Ng, Solving sparse non-negative tensor equations: Algorithms and applications, *Front. Math. China*, **10** (2015), 649–680. <https://doi.org/10.1007/s11464-014-0377-3>
3. Z. Luo, L. Qi, N. Xiu, The sparsest solutions to \mathcal{Z} -tensor complementarity problems, *Optim. Lett.*, **11** (2017), 471–482. <https://doi.org/10.1007/s11590-016-1013-9>
4. P. Azimzadeh, E. Bayraktar, High order Bellman equations and weakly chained diagonally dominant tensors, *SIAM J. Matrix Anal. A.*, **40** (2019), 276–298. <https://doi.org/10.1137/18M1196923>
5. H. He, C. Ling, L. Qi, G. Yhou, A globally and quadratically convergent algorithm for solving multilinear systems with \mathcal{M} -tensors, *J. Sci. Comput.*, **76** (2018), 1718–1741. <https://doi.org/10.1007/s10915-018-0689-7>

6. M. Liang, L. Dai, G. Zhou, Iterative methods for solving tensor equations based on exponential acceleration, *Numer. Algorithms*, **97** (2023), 29–49. <https://doi.org/10.1007/s11075-023-01692-w>
7. L. Han, A homotopy method for solving multilinear systems with \mathcal{M} -tensors, *Appl. Math. Lett.*, **69** (2017), 49–54. <https://doi.org/10.1016/j.aml.2017.01.019>
8. D. Li, S. Xie, H. Xu, Splitting methods for tensor equations, *Numer. Linear Algebr.*, **24** (2017), e2102. <https://doi.org/10.1002/nla.2102>
9. D. Liu, W. Li, S. Vong, The tensor splitting with application to solve multi-linear systems, *J. Comput. Appl. Math.*, **330** (2018), 75–94. <https://doi.org/10.1016/j.cam.2017.08.009>
10. W. Li, D. Liu, S. Vong, Comparison results for splitting iterations for solving multi-linear systems, *Appl. Numer. Math.*, **134** (2018), 105–121. <https://doi.org/10.1016/j.apnum.2018.07.009>
11. L. Cui, M. Li, Y. Song, Preconditioned tensor splitting iterations method for solving multi-linear systems, *Appl. Math. Lett.*, **96** (2019), 89–94. <https://doi.org/10.1016/j.aml.2019.04.019>
12. D. Liu, W. Li, S. Vong, A new preconditioned SOR method for solving multi-linear systems with an \mathcal{M} -tensor, *Calcolo*, **57** (2020), 15. <https://doi.org/10.1007/s10092-020-00364-8>
13. C. Lv, C. Ma, A Levenberg-Marquardt method for solving semi-symmetric tensor equations, *J. Comput. Appl. Math.*, **332** (2018), 13–25. <https://doi.org/10.1016/j.cam.2017.10.005>
14. M. Liang, B. Zheng, Y. Zheng, R. Zhao, A two-step accelerated Levenberg-Marquardt method for solving multilinear systems in tensor-train format, *J. Comput. Appl. Math.*, **382** (2021), 113069. <https://doi.org/10.1016/j.cam.2020.113069>
15. M. Liang, B. Zheng, R. Zhao, Alternating iterative methods for solving tensor equations with applications, *Numer. Algorithms*, **80** (2019), 1437–1465. <https://doi.org/10.1007/s11075-018-0601-4>
16. Y. Zhang, Y. Yang, N. Tan, B. Cai, Zhang neural network solving for time-varying full-rank matrix Moore-Penrose inverse, *Computing*, **92** (2011), 97–121. <https://doi.org/10.1007/s00607-010-0133-9>
17. Y. Xia, J. Wang, A recurrent neural network for nonlinear convex optimization subject to nonlinear inequality constraints, *IEEE T. Circuits-I*, **51** (2004), 1385–1394. <https://doi.org/10.1109/TCSI.2004.830694>
18. B. Qiu, J. Guo, M. Mao, N. Tan, A fuzzy-enhanced robust DZNN model for future multiconstrained nonlinear optimization with robotic manipulator control, *IEEE T. Fuzzy Syst.*, **32** (2023), 160–173. <https://doi.org/10.1109/TFUZZ.2023.3293834>
19. Y. Han, G. Cheng, B. Qiu, A triple-integral noise-resistant RNN for time-dependent constrained nonlinear optimization applied to manipulator control, *IEEE T. Ind. Electron.*, **72** (2024), 6214–6133. <https://doi.org/10.1109/TIE.2024.3482112>
20. B. Qiu, J. Guo, X. Li, Z. Zhang, Y. Zhang, Discrete-time advanced zeroing neurodynamic algorithm applied to future equality-constrained nonlinear optimization with various noises, *IEEE T. Cybernetics*, **52** (2020), 3539–3552. <https://doi.org/10.1109/TCYB.2020.3009110>
21. Q. Liu, J. Wang, A projection neural network for constrained quadratic minimax optimization, *IEEE T. Neur. Net. Lear.*, **26** (2015), 2891–2900. <https://doi.org/10.1109/TNNLS.2015.2425301>
22. Y. Xia, J. Wang, D. Hung, Recurrent neural networks for solving linear inequalities and equations, *IEEE T. Circ. Syst. Fundam.*, **46** (1999), 452–462. <https://doi.org/10.1109/81.754846>

23. B. Zhou, Finite-time stabilization of linear systems by bounded linear time-varying feedback, *Automatica*, **113** (2020), 108760. <https://doi.org/10.1016/j.automatica.2019.108760>
24. Y. Zhang, B. Liao, G. Geng, GNN model with robust finite-time convergence for time-varying systems of linear equations, *IEEE T. Syst. Man Cy.-S.*, **54** (2024), 4786–4797. <https://doi.org/10.1109/TSMC.2024.3387023>
25. L. Xiao, Z. Zhang, S. Li, Solving time-varying system of nonlinear equations by finite-time recurrent neural networks with application to motion tracking of robot manipulators, *IEEE T. Syst., Man, Cy.-S.*, **49** (2018), 2210–2220. <https://doi.org/10.1109/TSMC.2018.2836968>
26. X. Xiao, D. Fu, G. Wang, S. Liao, Y. Qi, H. Huang, et al., Two neural dynamics approaches for computing system of time-varying nonlinear equations, *Neurocomputing*, **394** (2020), 84–94. <https://doi.org/10.1016/j.neucom.2020.02.011>
27. M. Kharrat, Neural networks-based adaptive fault-tolerant control for stochastic nonlinear systems with unknown backlash-like hysteresis and actuator faults, *J. Appl. Math. Comput.*, **70** (2024), 1995–2018. <https://doi.org/10.1007/s12190-024-02042-2>
28. S. Qiao, X. Wang, Y. Wei, Two finite-time convergent Zhang neural network models for time-varying complex matrix Drazin inverse, *Linear Algebra Appl.*, **542** (2018), 101–117. <https://doi.org/10.1016/j.laa.2017.03.014>
29. X. Wang, Y. Wei, P. S. Stanimirović, Complex neural network models for time-varying Drazin inverse, *Neural Comput.*, **28** (2016), 2790–2824. <https://doi.org/10.1162/NECO-a-00866>
30. Y. Zhang, J. Zhang, J. Weng, Dynamic Moore-Penrose inversion with unknown derivatives: Gradient neural network approach, *IEEE T. Neur. Net. Lear.*, **34** (2022), 10919–10929. <https://doi.org/10.1109/TNNLS.2022.3171715>
31. S. Qiao, Y. Wei, X. Zhang, Computing time-varying ML-weighted pseudoinverse by the Zhang neural networks, *Numer. Func. Anal. Opt.*, **41** (2020), 1672–1693. <https://doi.org/10.1080/01630563.2020.1740887>
32. Y. Zhang, S. Ge, Design and analysis of a general recurrent neural network model for time-varying matrix inversion, *IEEE T. Neural Networ.*, **16** (2005), 1477–1490. <https://doi.org/10.1109/TNN.2005.857946>
33. Y. Zhang, S. Li, J. Weng, B. Liao, GNN model for time-varying matrix inversion with robust finite-time convergence, *IEEE T. Neur. Net. Lear.*, **35** (2022), 559–569. <https://doi.org/10.1109/TNNLS.2022.3175899>
34. Y. Shen, P. Miao, Y. Huang, Y. Shen, Finite-time stability and its application for solving time-varying Sylvester equation by recurrent neural network, *Neural Process. Lett.*, **42** (2015), 763–784. <https://doi.org/10.1007/s11063-014-9397-y>
35. M. Zhang, B. Zheng, Accelerating noise-tolerant zeroing neural network with fixed-time convergence to solve the time-varying Sylvester equation, *Automatica*, **135** (2022), 109998. <https://doi.org/10.1016/j.automatica.2021.109998>
36. Q. Hu, B. Zheng, An efficient takagi-sugeno fuzzy zeroing neural network for solving time-varying Sylvester equation, *IEEE T. Fuzzy Syst.*, **31** (2022), 2401–2411. <https://doi.org/10.1109/TFUZZ.2022.3225630>

37. Q. Hu, B. Zheng, An efficient and robust varying-parameter projection neural network for sparse signal reconstruction, *Neurocomputing*, **579** (2024), 127939. <https://doi.org/10.1016/j.neucom.2024.127939>
38. C. Han, J. Xu, B. Zheng, A second-order projection neurodynamic approach with exponential convergence for sparse signal reconstruction, *Appl. Soft Comput.*, **165** (2024), 112044. <https://doi.org/10.1016/j.asoc.2024.112044>
39. Y. N. Zhang, D. C. Jiang, J. Wang, A recurrent neural network for solving Sylvester equation with time-varying coefficients, *IEEE T. Neural Networ.*, **13** (2002), 1053–1063. <https://doi.org/10.1109/TNN.2002.1031938>
40. X. Wang, M. Che, Y. Wei, Neural networks based approach solving multi-linear systems with \mathcal{M} -tensors, *Neurocomputing*, **351** (2019), 33–42. <https://doi.org/10.1016/j.neucom.2019.03.025>
41. S. Wang, L. Jin, X. Du, P. S. Stanimirovi, Accelerated convergent zeroing neurodynamics models for solving multi-linear systems with \mathcal{M} -tensors, *Neurocomputing*, **458** (2021), 271–283. <https://doi.org/10.1016/j.neucom.2021.06.005>
42. M. Liu, H. Wu, M. Shang, A noise-suppressing discrete-time neural dynamics model for solving time-dependent multi-linear \mathcal{M} -tensor equation, *Neurocomputing*, **520** (2023), 240–249. <https://doi.org/10.1016/j.neucom.2022.11.071>
43. X. Wang, M. Che, Y. Wei, Neural network approach for solving nonsingular multi-linear tensor systems, *J. Comput. Appl. Math.*, **368** (2020) 112569. <https://doi.org/10.1016/j.cam.2019.112569>
44. X. Wang, C. Mo, M. Che, Y. Wei, Accelerated dynamical approaches for finding the unique positive solution of \mathcal{KS} -tensor equations, *Numer. Algorithms*, **88** (2021), 1787–1810. <https://doi.org/10.1007/s11075-021-01095-9>
45. Y. Zhang, C. Yi, D. Guo, J. Zheng, Comparison on Zhang neural dynamics and gradient-based neural dynamics for online solution of nonlinear time-varying equation, *Neural Comput. Appl.*, **20** (2011), 1–7. <https://doi.org/10.1007/s00521-010-0452-y>
46. L. Qi, Eigenvalues of a real supersymmetric tensor, *J. Symb. comput.*, **40** (2005), 1302–1324. <https://doi.org/10.1016/j.jsc.2005.05.007>
47. L. Lim, *Singular values and eigenvalues of tensors: A variational approach*, In: CAMSAP'05: Proceedings of IEEE International Workshop on Computational Advances in Multi-Sensor Adaptive Processing, Puerto Vallarta, Mexico, 2005, 129–132. <https://doi.org/10.1109/CAMAP.2005.1574201>
48. Y. N. Yang, Q. Z. Yang, Further results for Perron-Frobenius theorem for nonnegative tensors, *SIAM J. Matrix Anal. A.*, **31** (2010), 2517–2530. <https://doi.org/10.1137/090778766>
49. A. Polyakov, Nonlinear feedback design for fixed-time stabilization of linear control systems, *IEEE T. Automat. Contr.*, **57** (2012), 2106–2110. <https://doi.org/10.1109/TAC.2011.2179869>



AIMS Press

©2025 the Author(s), licensee AIMS Press. This is an open access article distributed under the terms of the Creative Commons Attribution License (<http://creativecommons.org/licenses/by/4.0>)